J. Plasma Physics (2000), *vol.* 63, *part* 2, *pp.* 115–128. Printed in the United Kingdom
© 2000 Cambridge University Press

Arc-liberated chemical energy exceeds electrical input energy

PETER GRANEAU,[1] NEAL GRANEAU,[2]
GEORGE HATHAWAY[3] and RICHARD L. HULL[4]

[1] Centre for Electromagnetics Research, Northeastern University, Boston, MA 02115, USA
[2] Department of Engineering Science, University of Oxford, Oxford OX1 3PJ, UK
[3] Hathaway Consulting Services, 39 Kendal Avenue, Toronto, Ontario, Canada M5R 1L5
[4] Tesla Coil Builders of Richmond, 7103 Hermitage Road, Richmond, VA 23228, USA

(Received 11 December 1998 and in revised form 5 August 1999)

Abstract. This paper reports the first experimental results in which the kinetic energy of cold fog, generated in a water arc plasma, exceeds the electrical energy supplied to form and maintain the arc. The cold fog explosion is produced by breaking down a small quantity of liquid water and passing a kiloampere current pulse through the plasma. The 90-year history of unusually strong water arc explosions is reviewed. Experimental observations leave little doubt that internal water energy is being liberated by the sudden electrodynamic conversion of about one-third of the water to dense fog. High-speed photography reveals that the fog expels itself from the water at supersonic velocities. The loss of intermolecular bond energy in the conversion from liquid to fog must be the source of the explosion energy.

1. Research motivation

Before describing the latest experiments concerned with cold fog explosions, the motivation for this research will be explained. In 1994, we discovered that when a small quantity of water (usually but not necessarily distilled) is converted to high-density fog within microseconds, the fog explodes violently. Fog is defined as a multiplicity of tiny water droplets that float in air. The discovery has been fully described in a book dealing with pre-Maxwellian electrodynamics (Graneau and Graneau 1996). More recent findings have been discussed in a previous paper in this journal (Hathaway et al. 1998).

The fog generator is a small water-filled electric arc cavity to be described later. In a typical explosion, the cavity receives less than about 50 J of electrostatic energy from a high-voltage capacitor. Almost all of the input energy is converted to low-grade heat, raising the water to a few degrees above ambient temperature. This heat is incapable of raising steam or contributing in any other way to the explosion. It seems inevitable that the fog is being produced by electrodynamic forces in the current-carrying arc plasma. Such forces can furnish the mechanical surface-tension energy required for tearing bulk water apart into tiny fog droplets.

With 50 J of input energy, the quantity of fog produced is of the order of 0.75 g of water. To dissociate this amount of water into oxygen and hydrogen would require 10 kJ of energy. Hence the fog explosion is unlikely to be caused

https://doi.org/10.1017/S002237789900817X Published online by Cambridge University Press

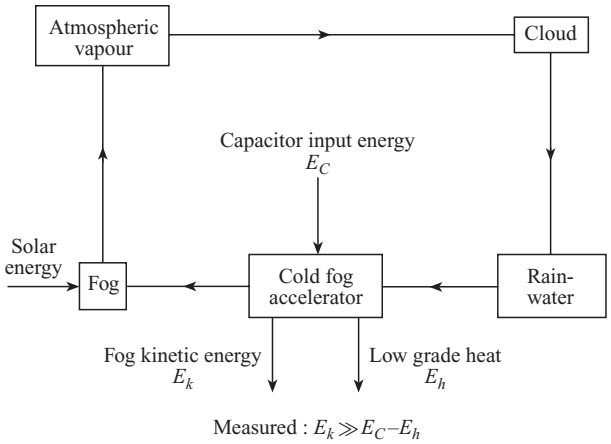


Figure 1. Renewable water energy cycle.

by electrolytic dissociation of water molecules. Without this dissociation, the most likely source of the explosion energy is that stored by hydrogen bonds between the water molecules. This bond energy is said to be equal to the latent heat of evaporation, and therefore could contribute up to 2200 J g^{-1}.

Figure 1 depicts the proposed renewable water energy cycle. The fog contains less H_2O–H_2O bond energy per gram than a raindrop. In other words, its latent heat of evaporation is less than that of bulk water. This is known from the fact that the equilibrium vapour pressure just outside a water droplet increases with decreasing droplet diameter (Young 1993). The internal-energy difference between the cold fog expelled from the accelerator must be made up by atmospheric heat – that is, essentially by solar energy. No other energy source appears to be available for replacing the extracted kinetic energy.

2. History of water arc explosions

It appears that the encounter of water drops with an electric arc produced the first photograph of a cold fog explosion. This is shown in Fig. 2, which was published by Trowbridge (1907). He must have realized that steam and water vapour were invisible in air, which left him with no explanation of the white explosion cloud. In his early high-voltage laboratory at Harvard University, Trowbridge discovered another effect that has a bearing on fog explosions. He stretched a sheet of paper along the path of his sparks of more than 50 cm length, and found that at every corner and forking of the lightning-like discharge, holes were punched through the paper without any burning or charring. It took 80 years until experiments of this kind were repeated at MIT and revealed that thunder was not the result of heat and the thermal expansion of the lightning channel (Graneau 1989), as had been assumed during most of the 20th century. It was shown instead that the shock wave in air was driven by non-thermal forces, of which electrodynamic forces were then considered to be the most likely. In view of the findings reported in the present paper, it is possible that cold fog explosions also contribute to the mechanism that causes thunder.

https://doi.org/10.1017/S002237789900817X Published online by Cambridge University Press



Figure 2. Trowbridge's (1907) photograph of a cold fog explosion. The arc is ~ 40 cm long.

During the Second World War, Frungel (1948) measured the unusual strength of water arc explosions. He concluded that the explosions were not caused by heat and steam, and admitted freely that he was unable to explain the phenomenon.

Soon after Frungel's publications, water arc explosions found applications in electrohydraulic metal forming (Gilchrist & Crossland 1967) and underwater pulse echo sounding (Frungel 1965). Not until the mid-1980s was the scientific basis of the puzzling explosions more extensively researched at MIT (Azevedo et al. 1986). It was then shown that the discharge of 3.6 kJ of stored capacitor energy would create pressures in excess of 20000 atm, in 7 ml of saltwater: 3.6 gm of water was ejected from the accelerator barrel with a velocity of the order of 1000 m s^{-1}, and then punched a $\frac{1}{2}$-inch-diameter hole through a $\frac{1}{4}$-inch-thick aluminium plate (Graneau and Graneau 1996).

At the time, it was conjectured that the water was flying through the air as

https://doi.org/10.1017/S002237789900817X Published online by Cambridge University Press

a coherent liquid slug, since that would create the greatest impact. No evidence of boiling and steam formation could be detected, and all the water found after the explosion was cool. Accepting the general view that plasmas are quasineutral and do not explode as a result of Coulomb forces, the available evidence seemed to leave little doubt that the explosions were driven by electrodynamic forces. This discovery motivated a 10-year investigation of the electrodynamics of water arcs. The Lorentz force could not account for more than a small fraction of the observed force. Ampère's force law (Graneau and Graneau 1996) fared better, but still fell short of predicting the measured values by at least a factor of 10. The search for a new electrodynamic force was finally abandoned in 1994.

Another report of electrically induced explosions in water came from Kansas State University. Johnson (1992) claimed that the loudness was distinctly greater than that obtained with an equivalent amount of gunpowder. He found that the remaining water droplets were cool to the touch and that apparently no steam had been produced. Johnson suggested that the explosions may have been due to longitudinal Ampère forces, and were tapping a new source of energy.

In 1994, the present authors took the first high-speed photographs of water ejected from an arc accelerator, and discovered that the leading high-speed component was not a coherent liquid, but actually very dense fog, which finally expanded in the air under the laboratory ceiling. By trapping the fog in a balsa-wood absorber and measuring its temperature, it was found that the fog was still cold – at most a few degrees above ambient temperature. The discovery of cold fog explosions changed our scientific outlook on the remarkable behaviour of water arcs.

3. Accelerator and discharge circuit

Our experimental technique and many previous results were published in Graneau and Graneau (1996) and Hathaway et al. (1998). Here we cite later results together with brief details of the relevant accelerator and discharge circuit as well as the diagnostics involved.

Figure 3 shows a cross-section though the Type A accelerator which has been used extensively since 1984. During this period, it has been made of different materials and has employed a variety of water charge volumes w and breech-to-muzzle lengths l. For example, fog penetration of a $\frac{1}{4}$-inch-thick aluminium plate was achieved with an accelerator using a steel barrel of $l = 10$ cm and $w = 7$ ml of saltwater. Subsequent shots have not used saltwater. In the latest experiments reported in this paper, the shaded metal components were made of copper and the remainder was a nylon sleeve and a nylon block. The essential dimensions are indicated on Fig. 3, with, typically $l = 3.0$ cm and $w = 3.5$ ml of distilled water. The water level was 0.26 cm below the muzzle.

The secondary projectile stood on top of the muzzle, and consisted of a 2.65 cm diameter balsa-wood cylinder of 3.2 cm length pressed into a copper can to add strength and weight, making the dry secondary projectile mass approximately $M = 65$ g. Behind the accelerator stood a scale on which a video camera recorded the height h to which the wet mass $M + m$ ascended, where m is absorbed fog mass.

https://doi.org/10.1017/S002237789900817X Published online by Cambridge University Press

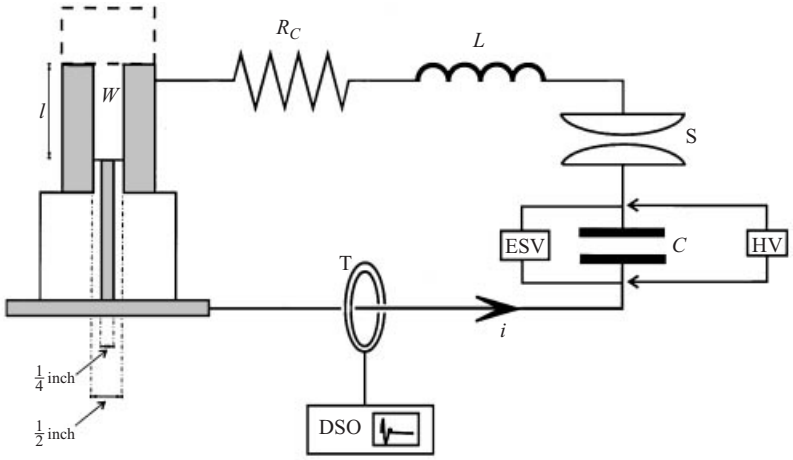


Figure 3. Type A accelerator with discharge circuit.

In a typical experiment, the energy storage capacitor $C = 0.565\ \mu\text{F}$ was connected between the barrel electrode and the baseplate-and-rod electrode. The switch S was a triggered spark gap in atmospheric air, which trapped a certain amount of residual charge in the capacitor when the switching arc interrupted the oscillating discharge at low current.

In Fig. 3, the distributed circuit resistance and inductance are indicated by lumped parameters R_C and L. The discharge current i was measured with a current transformer T and a digital storage oscilloscope DSO. The electrostatic voltmeter ESV recorded the charging voltage V_0 on the capacitor terminals with the switch S open, and the residual voltage V_r after the switch had been fired and then interrupted the current flow. With S open, the high-voltage power supply HV was connected across the capacitor for each shot. After reaching the desired voltage V_0, the supply was disconnected. Closing the switch S initiated the fog explosion, with the underdamped discharge current ringing down over a few microseconds.

4. Evidence of fog

That water arc explosions are in fact cold fog explosions was discovered with high-speed photography at Oxford University (Graneau and Graneau 1996; Hathaway et al. 1998). In the present paper, we are presenting further photographic evidence of fog generation that reveals interesting properties of the fog jets.

Figure 4 is a series of numbered photo frames showing the emergence of fog from the muzzle of a water arc accelerator as the fog pierces the atmosphere. The high-speed film was shot in the HCS Laboratory in Toronto at 35000 frames per second. A powerful light flash, triggered by the switch S of Fig. 3, was directed at the experimental apparatus. The camera formed images of the travelling fog on a rotating mirror, which reflected them to a film adhering to the inside of a rotating drum. The time interval between successive frames was 28.6 μs.

Water vapour is invisible in air. Relatively large water drops and films of water are transparent. They show up on photographs only because of thin lines

https://doi.org/10.1017/S002237789900817X Published online by Cambridge University Press

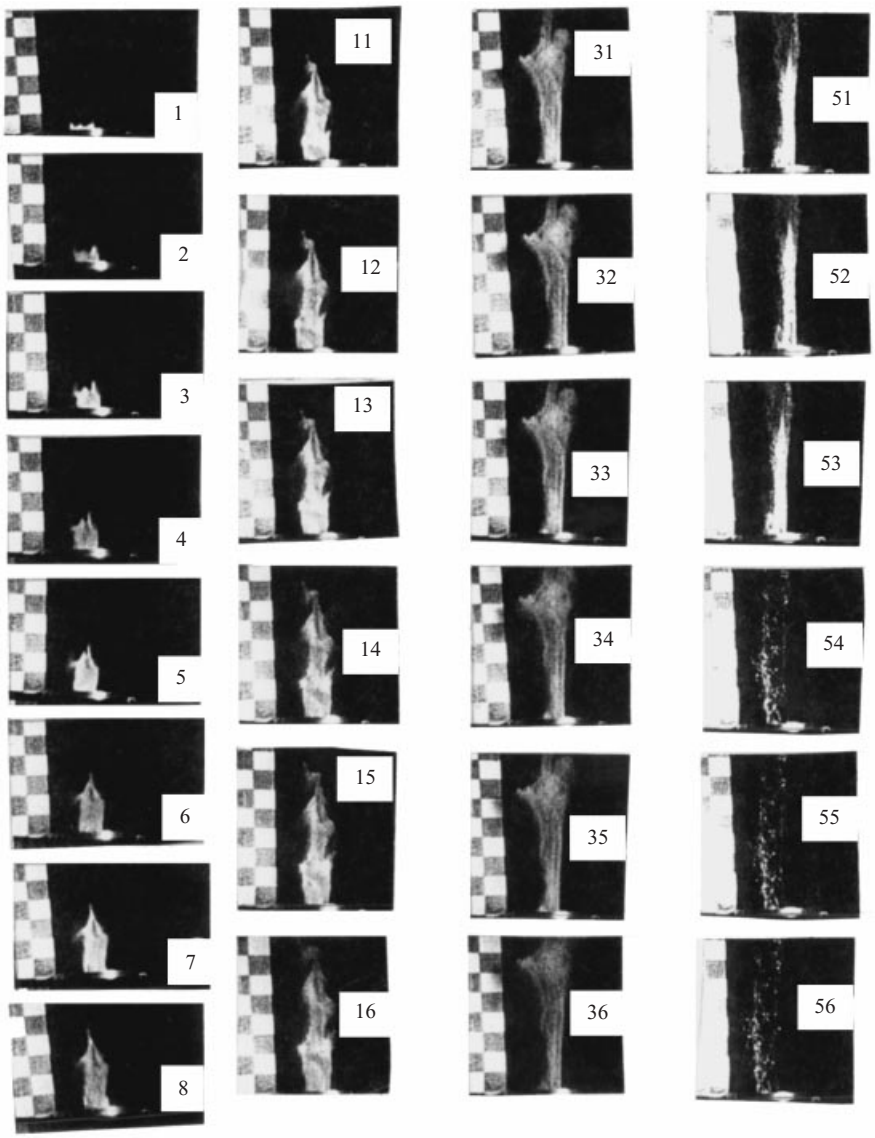


Figure 4. High-speed photography of a fog jet, 35000 frames per second.

of light that are reflections from the water surfaces. The uniform whitish-grey appearance of fog and clouds is due to light scattering by a multitude of small droplets. Hence the photographs in Fig. 4 conclusively prove the emergence of fog from the accelerator barrel. Video camera records, obtained in the laboratory of Tesla Coil Builders of Richmond (TCBOR), revealed that the fog slowed down quite rapidly as it penetrated the atmosphere. On reaching the ceiling, it rolled around like a cloud for a number of seconds while it evaporated.

When the accelerator depicted in Fig. 3 stood on an aluminium sheet spread out on the floor, it was observed that small droplets of mist rained out of the cloud. Fog droplets that float in air are said to be of diameters ranging from 1 to 100 μm. The fog recorded in Fig. 4 is likely to have contained some larger

https://doi.org/10.1017/S002237789900817X Published online by Cambridge University Press

droplets that fell in air, but, for the purpose of this paper, we shall call the mixture of very small floating and falling droplets 'high-density fog'. In other photographs (Graneau and Graneau 1996), larger drops of water were seen to follow behind the fog, some of which were millimetres in diameter and travelled at much lower velocities.

Figure 4 shows a selection of the nearly 200 frames recorded by the camera during a single shot. The fog column diameter just above the muzzle is equal to the accelerator barrel diameter, which was 1.27 cm. This immediately proves that the fog is cold and, unlike steam, does not expand laterally. A centimetre scale stands to the left of the fog column, and, by knowing the camera speed, the average velocity of the head of the fog column, taken over the first eight frames, was measured to be approximately 200 m s^{-1}. The fog appears to be coasting in the inertial mode. It is not understood why, initially, the column has a pointed tip, which would normally indicate supersonic speed (> 350 m s^{-1}). Anyhow, frames 11–16 show air ablation of the tip. By frames 31–36, a mushroom-shaped head has emerged with pronounced lateral fog spreading due to atmospheric ablation. Mushroom heads usually result from subsonic progression, and frames 31–36 demonstrate a velocity of 65 m s^{-1}.

The high-speed camera was triggered by the switch that initiated the arc discharge. This occurred no more than 28.6 μs before the exposure of frame 1. As the fog emerged from the muzzle, the explosion must have been over – otherwise it would have resulted in lateral fog expansion. This finding suggested that the explosion period was limited to the time during which the arc current was flowing, which was of the order of 10 μs. Heat could not have been the cause of the explosion, because this would have persisted for more than 28 μs.

The arc forms near the breech of the accelerator, located at the bottom of the water column. This is where the fog is likely to be generated. The water column in the barrel was 3 cm long. No water appears to have been pushed ahead of the fog, which initially may have travelled with a velocity as high as 1000 m s^{-1}. Other photographs have indicated that the fog breaks through the water surface without causing as much as a ripple. The implication is that the leading fog droplets are extremely small and spaced apart from each other. The smaller the droplets, the more bond energy per unit mass has been liberated and the more strongly the droplets should repel each other.

A transition from fog to transparent water begins to show in frames 51–53. Frames 181–185 depict a liquid flow at 15 m s^{-1}. The water in the latter frames must have been a hollow film tube with a few droplets in the surface, since normal-density liquid water could have only accounted for a 3 cm long solid column.

Figure 5 is a single frame taken with an ordinary video camera in the HCS Laboratory. In this case, the liberated chemical energy is much greater than in the high-speed film of Fig. 4. In Fig. 5, the fog plume is 2 m tall, and its shock-wave-shaped pointed tip very clearly travels at supersonic speed. This photograph reveals the light source about 50 cm to the right of the fog jet.

When a balsa-wood cylinder in a metal cup stood on the muzzle of the accelerator, the fog penetrated deep into the porous material and transferred momentum to the projectile, which was thrown vertically to a height h. Weighing before and after a shot made it possible to determine the dry mass M of the projectile and the absorbed fog mass m. Since the two masses travelled

https://doi.org/10.1017/S002237789900817X Published online by Cambridge University Press



Figure 5. Two-metre-tall supersonic fog jet. Approximate fog density 1 kg m^{-3}.

together at the initial projectile velocity v_0, momentum conservation required that

$$mu_{\mathrm{av}} = (M+m)v_0, \tag{1}$$

where u_{av} was the average velocity of the absorbed fog. Then it follows from energy conservation that

$$\tfrac{1}{2}(M+m)v_0^2 = (M+m)gh, \tag{2}$$

or

$$v_0 = \sqrt{2gh}, \tag{3}$$

where g is the acceleration due to gravity.

From (1) and (3), the average fog velocity can be calculated as

$$u_{\mathrm{av}} = \frac{M+m}{m}\sqrt{2gh}. \tag{4}$$

https://doi.org/10.1017/S002237789900817X Published online by Cambridge University Press

This average velocity gave the minimum kinetic energy of the fog as

$$E_{k,\min} = \tfrac{1}{2} m u_{\mathrm{av}}^2. \tag{5}$$

The true kinetic energy of the fog depends on the root-mean-square (rms) velocity of the droplets, because for n droplets of mass Δm travelling at velocity u, we have

$$E_k = \sum_n \tfrac{1}{2} \Delta m\, u^2 = \tfrac{1}{2} u_{\mathrm{rms}}^2 \sum_n \Delta m = \tfrac{1}{2} m u_{\mathrm{rms}}^2. \tag{6}$$

Sections cut from the balsa wood revealed that fog penetration varied widely from place to place. However, in general, the velocity distribution has the form of a half-cycle of a sine wave. The average ordinate of the sine wave is the amplitude divided by $\frac{1}{2}\pi$ and the rms value is the amplitude divided by 2, yielding

$$u_{\mathrm{rms}} = 1.1 u_{\mathrm{av}}. \tag{7}$$

The rms velocity is not very different from the average velocity, and (7) has been used in the evaluation of the fog kinetic energy.

5. Energy flow diagram

The energy flow through the discharge circuit and accelerator to the fog jet can be better understood with the aid of Fig. 6. The capacitor receives an energy E_1 from the high-voltage charging unit. Recognizing that a small amount of the energy remains in the capacitor, $E_2 < E_1$ is supplied to the discharge circuit, which is shown as separate from the accelerator. In the metallic components of the circuit and in the switching arc plasma, part of E_2 is dissipated as Ohmic heat E_3, which is proportional to i^2 and can be measured. For the purpose of Fig. 6, the ionization loss in the switch is added to the ionization loss in the water to give E_5, which contributes to the measured damping of the ringing discharge.

In addition to the absorbed ionization energy, which does not heat the water but is stored electrostatically until the ions recombine well after the explosion, some Ohmic heating of the water plasma takes place. This has been measured approximately with a thermocouple, and is labelled E_6.

Disregarding the fact that it is a plasma, the water itself acquires kinetic energy E_9, which is evidenced by the explosion. We let E_7 be the non-thermal mechanical energy required for tearing the liquid apart into fog droplets. Any liberated internal water energy E_8 may be added to E_7, and contributes to E_9. Before the kinetic energy of the fog jet E_{12} is measured, the fog has to penetrate a certain volume of liquid water, and is likely to dissipate some of its energy owing to viscous drag. This loss component is denoted by E_{11}. Whatever forces accelerate the fog in the water will also exert pressure on the cavity walls. The resulting strain and deformation energy stored temporarily in the wall material has been labelled E_{10}.

The critical quantity of the energy flow diagram is E_7. Measurements (Graneau and Graneau 1996) of E_3, E_5 and E_6 have established that $E_7 \ll E_2$. In the relevant experiment, E_2 was usually less than 50 J and the water quantity was never less than $w = 1$ ml. It follows from these figures that the water temperature could not exceed the ambient temperature by more than 12 °C. Furthermore, it was established by experiment with a photodiode that the arc

https://doi.org/10.1017/S002237789900817X Published online by Cambridge University Press

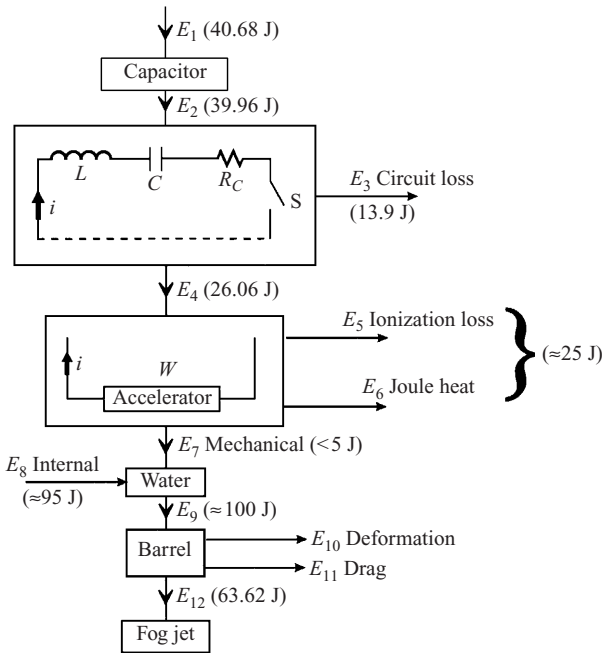


Figure 6. Energy flow diagram for shot TA70751.

current i was negligibly small until the water plasma was fully glowing in the accelerator barrel. Hence no selective subheating of a subvolume (filament) of w would have occurred. These facts determined once more that E_7 was not heat energy. It has to be electrodynamic energy associated with magnetic forces.

The numerical energy quantities in Fig. 6 apply to shot TA70751 of Table 1. Where estimates have been made, the figure is preceded by the 'approximate' symbol $\approx$. In all other cases, actual measurements are presented. The methods used for estimating and measuring energy losses are described more fully in Graneau and Graneau (1996). The estimated value of $E_5 + E_6 \approx 25$ J would produce a temperature rise in the 3.5 g of water in the accelerator of about 1.7 °C. This is consistent with temperature measurements made in other experiments.

It should be noted that in shot TA70751, the amount of fog absorbed in the balsa-wood secondary projectile was 0.537 g. If at any time this water mass had existed as steam, it would have required the expenditure of 1213 J, an amount equal to the latent heat of vaporization. However, the total energy discharged from the capacitor was only $E_2 = 40$ J. This was clearly insufficient to explain the explosion by the adiabatic expansion of steam.

The most intriguing feature of the energy flow diagram is the large magnitude of E_{12} as documented in the following section. This demands the supply of internal water energy E_8.

6. Fog kinetic-energy results

Table 1 lists the measured kinetic energy of the fog jets in eight shots fired under identical conditions with the Type A accelerator of Fig. 3. As already explained, almost all of the fog kinetic energy is derived from internal water

https://doi.org/10.1017/S002237789900817X Published online by Cambridge University Press

Table 1. Results of eight shots with the Type A accelerator, with $V_0 = 12.0$ kV, $V_r = 1.6$ kV, $C = 0.565$ μF, $E_2 = 39.96$ J $l = 3.0$ cm and $w = 3.5$ ml (distilled water).

Shot	M (g)	m (g)	h (m)	E_{12} (J)	E_{12}/E_2
TA70564	69.278	0.718	0.57	40.54	1.015
TA70565	65.363	0.608	0.58	50.18	1.256
TA70567	64.548	0.632	0.48	39.00	0.876
TA70568	64.200	0.621	0.56	45.80	1.146
TA70569	63.588	0.843	0.59	35.12	0.879
TA70570	65.481	0.659	0.58	46.54	1.165
TA70571	64.905	0.537	0.66	63.62	1.592
TA70572	63.660	0.823	0.54	32.98	0.825

energy, and $E_7 \ll E_2$. The results in Table 1 show that in five of the eight shots, the kinetic energy of the fog was greater than the energy supplied by the storage capacitor. In other words, we achieved $E_{12}/E_2 > 1$. The ratio E_{12}/E_2 is one of several markers indicating the release of internal water energy.

To appreciate how small the thermal action of the 40 J input energy is, it helps to think of an ordinary match, which liberates between 100–200 J of thermal energy. If this energy is used to heat 3.5 ml of water in a test tube, it will certainly not cause a water explosion, nor will it produce a noticeable lift of the water surface. This immediately suggests that E_7, which must be responsible for the fog explosion, has to be mechanical energy. In any case, the measured low-grade heat losses $E_3 + E_5 + E_6$ account for almost all of the input energy E_2 (Graneau and Graneau 1996), leaving very little for E_7.

Dielectric breakdown and ionization do not result in an explosion unless subsequently a significant amount of current flows through the arc plasma. This is supported by the fact that breakdown and ionization are energy-absorbing phenomena. The strong current dependence of the explosions was already demonstrated by Azavedo et al. (1986). In their work, lowering the maximum pulse current from 25 to 12 kA reduced the explosion impulse from 7.0 N s to 1.5 N s. Currents of less than 1000 A yielded negligible explosion forces. The ionization of water during the breakdown and plasma generation phase, as well as any Coulomb forces associated with charge separation, do not appear to be responsible for the arc explosions. This leaves only electrodynamic (magnetic) forces between current elements as the possible cause of the explosions. The strength of the explosions undoubtedly increases with the current i, and this is in accordance with electrodynamic processes.

If F is the time-varying force that accelerates the fog droplets then Newtonian mechanics requires that the impulse of this force, $\int F\,dt$, has to generate the initial fog momentum mu_{av}. Let a constant effective force F_e be defined, acting for an interval τ, such that it is equal to the impulse $\int F\,dt$. Then

$$\int F\,dt = F_e\tau = mu_{\mathrm{av}}. \tag{8}$$

The average velocity can be calculated from (4). The time constant τ of the underdamped discharge current will be assumed to be the interval during which F_e is active. In the absence of steam, it is difficult to see how the force pulse

https://doi.org/10.1017/S002237789900817X Published online by Cambridge University Press

could be stretched out beyond the length of the current pulse. The discharge current has the form

$$i = I_0 e^{-t/\tau} \sin \omega t, \tag{9}$$

where ω is the angular ringing frequency. From current oscillograms, a typical value of the time constant was $\tau = 4$ μs. This resulted in $F_e = 52400$ N for the weakest shot (TA70752) of Table 1, or an effective pressure over the cross-sectional area of the accelerator barrel of 4.14×10^8 N m^{-2}, which is equal to 4220 atm. This would appear to be sufficient pressure to achieve the observed fog acceleration.

Maxwell's electromagnetic field theory indicates that by far the strongest electrodynamic force on the plasma arc column is the magnetic pinch exerted by radial Lorentz forces. This produces an axial thrust that could expel water from the barrel. To make this force a maximum, we take the optimistic view that the current flows all in the axial direction. Northrup (1907) showed that the total axial thrust on a cross-section of a cylindrical current distribution is given by

$$F = \frac{\mu_0}{4\pi} \frac{i^2}{2}, \tag{10}$$

where μ_0 is the magnetic permeability of free space. The impulse of this pinch thrust can again be expressed by an effective force F_e such that

$$\int F \, dt = F_e \tau = \frac{\mu_0}{4\pi} \frac{1}{2} \int i^2 \, dt. \tag{11}$$

The action integral $\int i^2 \, dt$ was measured for many discharges, and a typical value was 130 A^2 s. With this information, the effective Lorentz thrust of (11) becomes $F_e = 1.6$ N, as compared with the force of 52 kN required to accomplish the observed fog acceleration.

Newtonian electrodynamics (Graneau and Graneau 1996), which was widely taught and used in the 19th century, gives a larger effective electrodynamic force, possibly as high as 60 N. This is, however, still far too low to explain the fog acceleration. The chance of accounting for the observed fog accelerations with electrodynamic forces is even worse than these figures indicate, since E_9, the true fog acceleration energy, must be greater than E_{12} because of deformation and drag losses, and could even be twice as large as the measured energy.

The considerations outlined in this section demonstrate that, quite apart from the fact that $E_{12}/E_2 > 1$, the observed fog explosions demand the supply of internal water energy.

7. Water-to-fog conversion

Condensation of water vapour in the atmosphere is the greatest fog producer on Earth. It is a relatively slow process, which cannot generate a sufficient amount of fog in a few microseconds to cause an arc explosion. In the early formative stage of a water arc, the fog density must approach that of liquid water, and is therefore up to 300000 times as great as the fog density of clouds (approximately 3 g m^{-3}).

https://doi.org/10.1017/S002237789900817X Published online by Cambridge University Press

It is difficult to think of any other way of creating the dense fog than by mechanically tearing the liquid apart into tiny fragments. These are the fog droplets, ranging in size from 1 to 100 μm in diameter or smaller. As discussed previously, the tearing force must be an electrodynamic force, but the direction of the Lorentz force is not such that it could split water into droplets. On the other hand, the Ampère force, or Ampère tension as it is often called, is well qualified to describe the break-up of the liquid.

The most well-known consequence of Ampère tension in metallic conductors is the phenomenon of wire fragmentation. In liquids and plasmas, it leads to plasma bead formation, which has been observed in plasma focus fusion, deuterium-fibre fusion and capillary fusion experiments. These phenomena are fully reviewed in Graneau and Graneau (1996). Hence it is not only possible but likely that Ampère tension will generate fog in water arc explosions.

Surface tension requires that tearing forces be involved in the breakup of the liquid. The surface tension γ of water at 20 °C is 72.75 dyn cm^{-1}. It turns out that surface tension energy per unit area has the same dimension as surface tension per unit edge and is numerically equal to it, so that

$$\gamma = 72.75 \text{ dyn cm}^{-1} = 72.75 \text{ erg cm}^{-2} = 72.75 \times 10^{-7} \text{ J cm}^{-1}. \tag{12}$$

The fog mass generated in the experiments of Table 1 varied between 0.537 g and 0.843 g. Let us evaluate the additional surface-tension energy required to convert 1 g of water into fog. If the drops are all of the same diameter d then the number density n of droplets generated will be

$$n = \frac{6}{\pi d^3}. \tag{13}$$

Fog droplets are said to be between 10^{-4} and 10^{-2} cm in diameter. Hence the number of droplets lies in the range from 1.9×10^6 to 1.9×10^{12} per gram. The total new surface energy E_s for drops of the same size is

$$E_s = \gamma n \pi d^2. \tag{14}$$

For the two extreme droplet diameters of 10^{-2} and 10^{-4} cm, this energy comes to 4.37 and 437 mJ respectively. Hence the part of E_7 in the energy flow diagram of Fig. 6 that must supply surface tension energy is only a fraction of one joule. The Ampère tension forces can comfortably meet this energy demand, and may have some strength left over for fog acceleration. These findings lead us to believe that Ampère tension is responsible for the conversion of liquid water into dense fog.

8. Energy conservation

If energy is to be conserved then the internal energy per unit mass of fog (see Fig. 1) has to be less than that of rainwater. During the explosions, the water molecules do not appear to undergo chemical changes; so the energy difference must be explained by a change in the intermolecular bond energy per unit mass. This reserve of energy is believed to be equal to the latent heat of evaporation, and, in the case of rain water, it comes to 2259 J gm^{-1}.

In shot TA70751 (see Table 1), 0.537 g of water was converted to fog. The latent heat of this amount of water is 1213 J. The measured fog kinetic energy

https://doi.org/10.1017/S002237789900817X Published online by Cambridge University Press

came to $E_{12} = 63.62$ J. This is just over 5% of the latent heat. Furthermore, extensive analysis presented in Graneau and Graneau (1996) and Azevedo et al. (1986) has demonstrated that electrodynamic forces could only amount for a negligible portion of the kinetic energy developed in arcs. Therefore almost all of the input energy E_2 (E_C in Fig. 1) is converted to low-grade heat, so that nearly all of E_{12} must have come from the 1213 J stored in the bulk water.

This calculation has ignored the E_{10} and E_{11} losses shown in Fig. 6. Hence the energy liberated in the water-to-fog conversion is greater than 5% of the stored energy, implying that the latent heat of the fog created by the accelerator contains less than 95% of the latent heat of bulk water. As demonstrated by (14), less than 1 J (0.1% of the latent heat) of the stored energy loss can be associated with additional surface tension energy acquired by the fog. Therefore the remainder must have resulted from differences in the water structure. How this average structure and the intermolecular bonding changes with the number of molecules in the droplet is a topic of physical chemistry that is a subject of intense research (Postorino et al. 1993; Li and Ross 1993; Li 1996). The difference in the latent heat between fog and bulk water is eventually restored by heat in the atmosphere, which allows the fog to condense and return to earth. Our investigation has not yet extended into the details of water structure, but the discovery of cold fog explosions will help in this direction.

References

Azevedo, R., Graneau, P., Millet, C. and Graneau, N. 1986 *Phys. Lett.* **117A**, 101.

Frungel, F. 1948 *Optik* **3**, 125.

Frungel, F. 1965 *High Speed Pulse Technology*, Vol. 2. Academic Press, New York.

Gilchrist, I. and Crossland, B. 1967 *IEEE Conference Publ.* No. 38 (December), 92.

Graneau, P. 1989 *J. Phys. D: Appl. Phys.* **22**, 1083.

Graneau, P. and Graneau, N. 1996 *Newtonian Electrodynamics*. World Scientific, New Jersey.

Hathaway, G., Graneau, P. and Graneau, N. 1998 *J. Plasma Phys.* **60**, 775.

Johnson, G. L. 1992 In: *Intersociety Energy Conversion Engineering Conference Proceedings, San Diego, CA*, p. 335. IEEE Press, New York.

Li, J. and Ross, D. K. 1993 *Nature* **365**, 327.

Li, J. 1996 *J. Chem. Phys.* **105**, 6733.

Northrup, E. F. 1907 *Phys. Rev.* **24**, 474.

Postorino, P., Tromp, R. H., Ricci, M. A., Soper, A. K. and Nellson, G. W. 1993 *Nature* **366**, 668.

Trowbridge, J. 1907 *Mem. Am. Acad. Arts Sci.* **13**(5), 185.

Young, K. C. 1993 *Microphysical Processes in Clouds*. Oxford University Press.

https://doi.org/10.1017/S002237789900817X Published online by Cambridge University Press